Inorg. Chem. **2007**, *46*, 7403–7409

Silver Telluride Nanotubes Prepared by the Hydrothermal Method

Aimiao Qin,[†] Yueping Fang,*[,†] Pingfang Tao,[†] Jianyong Zhang,[‡] and Chengyong Su*[,‡]

School of Chemistry and Chemical Engineering, Guangxi Normal University, Guilin, Guangxi, 541004, China, and Key Laboratory of Bioinorganic and Synthetic Chemistry of MOE and State Key Laboratory of Optoelectronic Materials and Technologies, School of Chemistry and Chemical Engineering, Sun Yat-Sen University, Guangzhou 510275, China

Received April 9, 2007

Silver telluride nanotubes have been prepared by the hydrothermal process without a template or a surfactant. The as-prepared sample was characterized by X-ray diffraction, transmission electron microscopy, X-ray photoelectron spectra, and Raman spectra. The structural phase transition of the sample was observed. A rolling-up mechanism is proposed to explain the formation of the silver telluride nanotubes based on the inherent crystal structure of low-temperature β-Ag_2Te. Raman spectra analysis revealed an interesting Raman scattering enhancement phenomenon.

Introduction

Silver telluride exhibits some unique properties such as a structural phase transition and superionic conductivity. At about 145 °C,[1,2] silver telluride undergoes a structural phase transition from the low-temperature monoclinic structure (β-Ag_2Te) to the high-temperature face-centered cubic structure (α-Ag_2Te). The low-temperature β-Ag_2Te is a narrow band gap semiconductor[3] with high electron mobility and low lattice thermal conductivity. While in the high-temperature face-centered cubic structure (α-Ag_2Te), tellurium anions form a face-centered cubic sublattice through which Ag^+ cations can move easily and show superionic conductivity.[4,5] Recently, both silver-rich (n-type) and tellurium-rich (p-type) silver telluride bulk samples[6,7] or thin films[8] have been discovered to have large positive magnetoresistance, among which n-type silver telluride has specially remarkable magnetoresistance effects at room temperature and its linear field dependence is down to a few Øersteds.[6,7] Therefore, silver telluride could be a promising material for application in low-magnetic-field sensors. Along with the increasing interest in nanostructured materials and nanodevices, it becomes essential to fabricate silver telluride into different tiny units, such as 1D nanotubes, which are able to be applied on a nanoscale field.

Conventionally, metal chalcogenide was prepared by metallurgical processing by mixing appropriate amounts of pure elements at high temperatures.[9] More recently, some studies have been reported on the thermoelectric properties of silver telluride[8,10] and the synthesis of silver telluride nanofibers.[5,11,12] However, previously there have been no accounts of the synthesis and characterization of silver telluride nanotubes. Here, we report the synthesis and characterization of silver telluride nanotubes obtained by the hydrothermal process, without any template and surfactant. To the best of our knowledge, this is the first report of the preparation of silver telluride nanotubes by the hydrothermal method, which have emerged as powerful tools for the fabrication of anisotropic 1D nanomaterials.[13−17] The as-prepared samples were characterized by X-ray diffraction

* To whom correspondence should be addressed. E-mail: fyp66115@tom.com, Tel: 86-773-5821167, Fax: 86-773-5803930 (Y.P); E-mail: cesscy@mail.sysu.edu.cn (C.S.)..

[†] Guangxi Normal University.

[‡] Sun Yat-Sen University.

(1) Binary Alloy Phase Diagrams, ASM International. CDROM. 2nd ed.
(2) Martin, C. R. *Science* **1994**, *266*, 1961.
(3) Dalven, R.; Gill, R. *J. Appl. Phys.* **1967**, *38*, 753.
(4) Kobayashi, M.; Ishikawa, K.; Tachibana, F.; Okazaki, H. *Phys. Rev. B* **1988**, *38*, 3050.
(5) Chen, R.; Xu, D.; Guo, G.; Gui, L. *J. Mater. Chem.* **2002**, *12*, 2435.
(6) Xu, R.; Husmann, A.; Rosenbaum, T. F.; Saboungi, M. L.; Enderby, J. E.; Littlewood, P. B. *Nature* **1997**, *390*, 57.
(7) Schnyders, H. S.; Saboungi, M. L.; Rosenbaum, T. F. *Appl. Phys. Lett.* **2000**, *76*, 1710.
(8) Chuprakov, I. S.; Dahmen, K. H. *Appl. Phys. Lett.* **1998**, *72*, 2165.
(9) Coustal, R. *J. Chem. Phys.* **1958**, *38*, 277.
(10) Fujikane, M.; Kurosaki, K.; Muta, H.; Yamanaka, S. *J. Alloys Compd.* **2005**, *393*, 299.
(11) Mu, L.; Wan, J. X.; Ma, D. K.; Zhang, R.; Yu, W. C.; Qian, Y. T. *Chem. Lett.* **2005**, *34*, 52.
(12) Zhang, L.; Yu, J. C.; Mo, M.; Wu, L.; Kwong, K. W.; Li, Q. *Small* **2005**, *1*, 349.
(13) He, Z. B.; Yu, S. H.; Zhu, J. P. *Chem. Mater.* **2005**, *17*, 2785.
(14) He, Z. B.; Yu, S. H. *J. Phys. Chem. B* **2005**, *109*, 22740.
(15) Joshi, U. A.; Lee, J. S. *Inorg. Chem.* **2007**, *46*, 3176.

10.1021/ic7006793 CCC: $37.00
Published on Web 07/31/2007

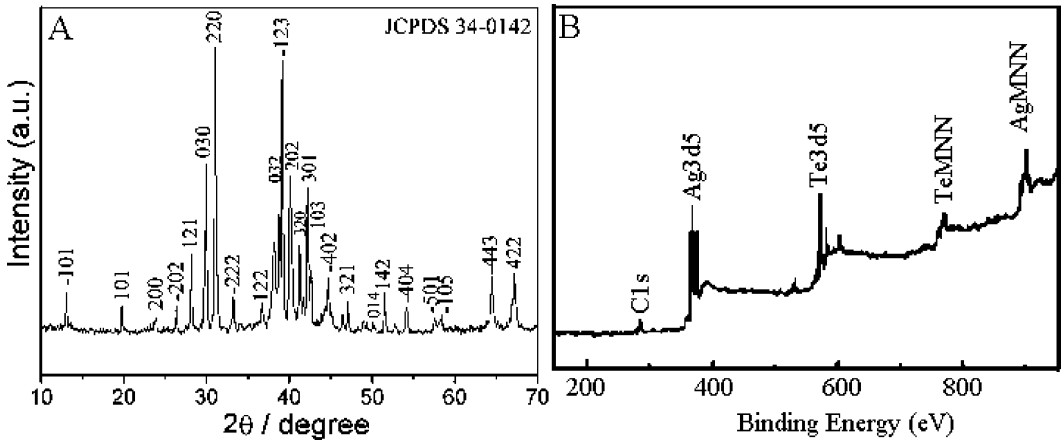

Figure 1. A) XRD pattern of as-prepared sample; B) XPS spectra of the as-prepared sample.

(XRD), transmission electron microscopy (TEM), high-resolution TEM (HRTEM), X-ray photoelectron spectra (XPS), and Raman spectra. The structural phase transition of the silver telluride nanotubes was observed. The rolling-up mechanism of the silver telluride nanotubes is also discussed on the basis of the inherent crystal structure of low-temperature β-Ag_2Te.

Experimental Section

In a typical procedure, 2 mmol of silver nitrate was dissolved in 24 mL of distilled water, and 1 mmol of sodium tellurate (Na_2TeO_3) was added with stirring. To this resulting solution, 1.5 mL of aqueous hydrazine solution (50%) and 0.5 mL of ammonia (25%) were dropped quickly in turn, and the mixture was transferred into a Teflon-lined autoclave (30 mL), heated to 120 °C, and maintained at this temperature for 12 h. After the hydrothermal treatment, the precipitate was collected and rinsed with distilled water and ethanol and then dried in air for further characterization.

The obtained products were directly subjected to scanning electron microscopy characterizations (SEM, JEOL JSM-6700F at an accelerating voltage of 5−15 kV) and powder-X-ray diffraction (XRD, Philips PW-1830 and Bruker AXS D8 ADVANCE X-ray diffractometer). The room-temperature Raman spectra of the Ag_2Te nanotubes were recorded with a micro-Raman spectrometer (Renishaw 1000, U.K.) equipped with a CCD detector and an Ar^+ laser with a 514.5 nm excitation line (diameter of laser spot, ~3 μm) and 4.2 mW of power. Thermogravimetric analyses were carried out on a NETZSCH TG 209 Instrument under flowing nitrogen. Differential scanning calorimetry (DSC) analysis was carried out up to a temperature of 250 °C, using a Mettler DSC-301 under a stream of nitrogen and a heating rate of 5 °C /min. X-ray photoelectron spectroscope (XPS) analysis was carried out on a VGESCALAB MK II X-ray photoelectron spectrometer, using non-monochromatized Mg Kα radiation as the excitation source and choosing C1 s (284.60 eV) as the reference line. For the transmission electron microscopic (TEM, JEOL 2010F microscopes operated at an accelerating voltage of 200 kV) observations, the product was sonicated in ethanol for 20 min, and the suspension was dropped onto a carbon-coated copper grid, followed by evaporation of the solvent in the ambient environment.

Results and Discussion

Crystal structures and compositions of the products have been determined by powder-XRD, and a typical result is shown in part A of Figure 1. The XRD pattern of the as-prepared sample can be readily indexed according to the monoclinic Ag_2Te crystal structure (JCPDS 34−0142) [space group: $P2/n$ (No. 13)]. The XPS spectra of Ag_2Te (part B of Figure 1) show that the binding energies of Ag3d5 and Te3d are 368.52 and 573.08 eV, respectively. The molar ratio of silver to tellurium according to the quantification of peaks is 2.000:1.034, close to the stoichiometry of Ag_2Te.

The morphology and structure of the samples were examined with scanning electron microscopy (SEM) and TEM. SEM images are shown in Figure 2. Numerous nanofibers as an entangled mesh are formed. All of the nanofibers are bendy and curled, with the diameters of 80−250 nm and more than several tens of micrometers in length (A and B). The nanofibers also show the characteristics of tubular structures with open-ended (C and D) and uncovered hollow interiors (E). More-detailed structural information about the nanofibers of the as-prepared sample is obtained from TEM studies. As shown in Figure 3, the curled nanofibers have the characteristics of tubular structure (A, C, and D) and always have at least one of the ends open. These nanotubes are single-crystalline and free of dislocation and stacking faults, as revealed by HRTEM analysis (B). A typical HRTEM image (B) taken from the white square in part A of Figure 3 exposes clear lattice fringes of {001} planes perpendicular to the tube axis with a d spacing of 0.736 nm. The fast Fourier transform (FFT) pattern (inset in part B of Figure 3) can be indexed to the monoclinic β-Ag_2Te, and the nanotubes grow along the [001] direction of the β-Ag_2Te crystal. X-ray energy-dispersive spectroscopy (EDS) gives an elemental ratio of silver to tellurium of about 2:1 and indicates that the nanotubes are made up of Ag_2Te.

To examine the structural phase transition of the as-prepared Ag_2Te sample from the low-temperature monoclinic structure (β-Ag_2Te) to the high-temperature face-centered cubic structure (α-Ag_2Te), thermogravimetric analysis (TGA) and differential scanning calorimetry (DSC) curves of the Ag_2Te sample were recorded and shown in part A of Figure

(16) Zhang, L. Z.; Yu, J. C.; Mo, M. S.; Wu, L.; Li, Q.; Kwong, K. W. *J. Am. Chem. Soc.* **2004**, *126*, 8116.
(17) Ma, R. Z.; Bando, Y.; Sasaki, T. *J. Phys. Chem. B* **2004**, *108*, 2115.

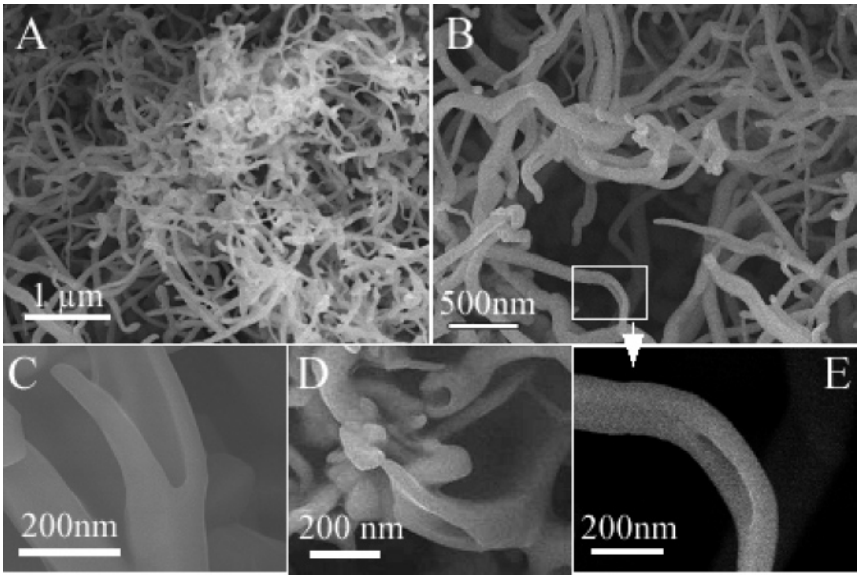

Figure 2. SEM images of as-prepared sample. (A) A lower magnification SEM image; (B) higher magnification SEM image; (C) and (D) tubular nanofibers with open ends; (E) tubular nanofiber with uncovered hollow interiors taken from the white square (B).

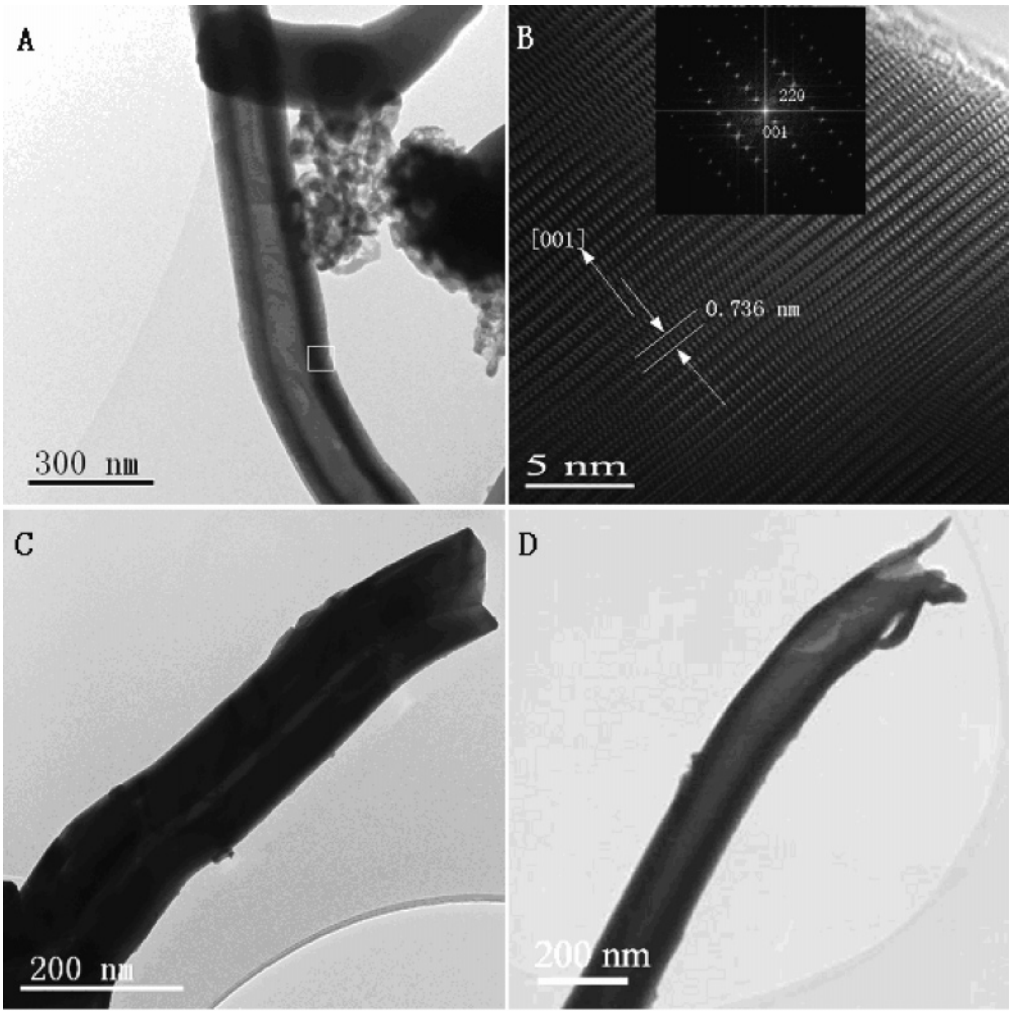

Figure 3. TEM images of the as-prepared sample: (A), (C), and (D) individual nanotube; (B) HRTEM image recorded from the white square in (A) and the corresponding FFT patterns (inset).

4. TGA (dot line) ranging from 100 to 200 °C did not show significant weight loss, indicating that the composition of the sample did not chemically change. From the DSC curve, it can be seen that the phase transition during the heating procedure occurred at 152.5 °C, whereas the reversible phase transition during the cooling procedure occurred at 140 °C.

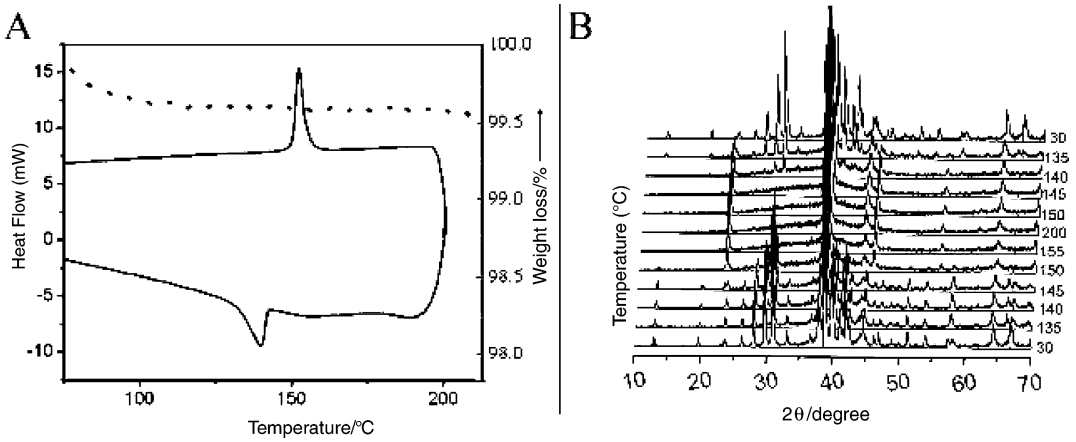

Figure 4. (A) TGA (dashed line) and DSC (solid line) curves of the as-prepared Ag_2Te sample; (B) The temperature-dependent XRD patterns of the as-prepared Ag_2Te sample.

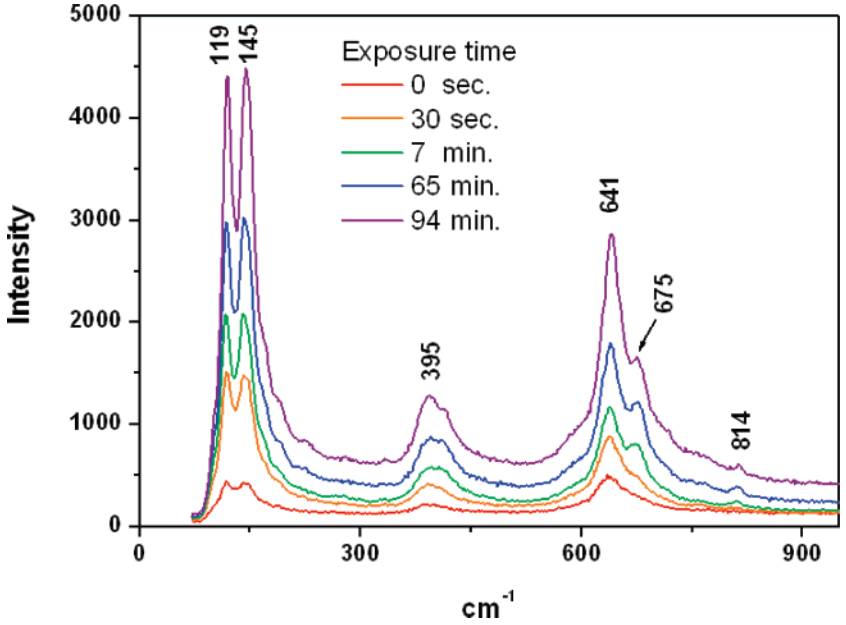

Figure 5. Raman scattering spectrum of the as-prepared Ag_2Te products at different times of exposure.

The DSC curve shows that the phase transition is indeed reversible, and there exists a hysteresis of ~12.5 °C. A similar hysteresis phenomenon has also been observed previously for the preparation and characterization of Ag_2E (E = Se, Te) nanocrystals, where the phase transition (at 148 °C) is also reversible but shows a hysteresis of 56 °C.[18] The temperature-dependent XRD patterns of the as-prepared Ag_2Te sample (part B of Figure 4) also show the structural phase transition from the low-temperature monoclinic structure (β-Ag_2Te) to the high-temperature face-centered cubic structure (α-Ag_2Te). From the temperature-dependent XRD patterns, it can be seen that the phase transition during the heating procedure occurred between 145 and 155 °C, whereas the reversible phase transition during cooling occurred between 145 and 135 °C. The temperature-dependent XRD patterns show that the phase transition is indeed reversible, and there exists a hysteresis of ~10 °C.

It is interesting that we observed the changed of the spectra the Ag_2Te nanotubes in the difference of the exposure time. At the very beginning, the intensity of the Raman spectra of Ag_2Te samples were rather weak as shown in Figure 5; however, as the samples were exposed to the laser for a longer time, the intensity of the Raman spectra became dramatically stronger, and the main peaks were sharpened when the exposure time was increased. The initial spectrum shows three weak peaks at 119, 145, and 641 cm^{-1}. As the exposure time is lengthened, two new peaks appear at 675 and 814 cm^{-1}. However, none of the above observed peaks are convincingly assignable to Ag−Te Raman vibrations.

Because silver chalcogenides are sensitive to laser beams, which may induce the polymorphic transitions and result in a redox reaction,[19] no studies have reported on the Raman spectra measurements of Ag_2Te. Here, we propose a tentative explanation of the Raman spectra. Upon exposure of the

(18) Harpeness, R.; Palchik, O.; Gedanken, A.; Palchik, V.; Amiel, S.; Slifkin, M. A.; Weiss, A. M. *Chem. Mater.* **2002**, *14*, 2094.

(19) Henshaw, G.; Parkin, I. P.; Shaw, G. A. *J. Chem. Soc., Dalton Trans.* **1997**, 231.

Scheme 1. Perfective Projection Along the *b* and *c* Axes of the Structure of β-Ag_2Te

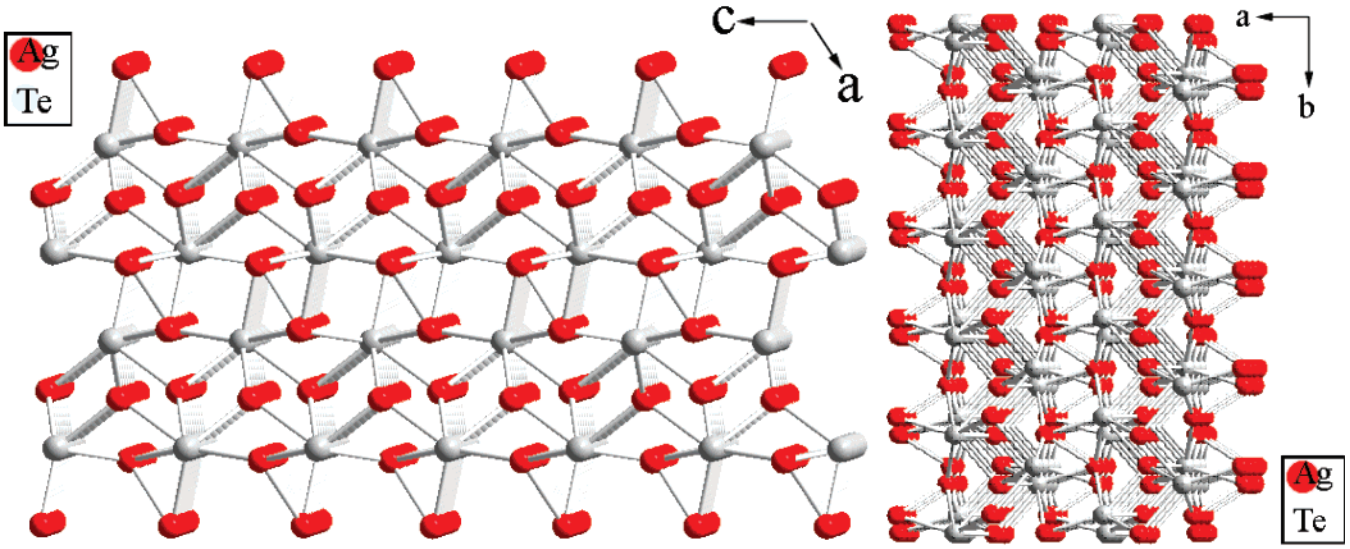

surface of Ag_2Te to the laser, nanotubes may undergo a redox reaction, resulting in trace amounts of TeO_2 and silver. The redox reaction takes place on the surface of the sample and is expressed as

$$Ag_2Te + O_2 = 2Ag + TeO_2$$

The legible Raman vibrations are possibly due to the appearance of TeO_2, with the peaks at low frequency (<200 cm^{-1}) corresponding to the lattice vibrations of TeO_2, those at 395 and 641 cm^{-1} corresponding to the bending vibrations, and those at 675 and 814 cm^{-1} corresponding to the symmetrical stretching of Te−O.[20] The Raman scattering was weak at the beginning because such laser-induced decomposition only produced very little TeO_2. However, the concomitant appearance of silver still made it detectable by Raman. When the sample was exposed to the laser for a longer time, more and more silver atoms were generated, and the Raman intensity increased dramatically, which exhibited a significant enhancement of the Raman spectra. In the meantime, such Raman enhancement may be able to activate some originally non-Raman active modes, accounting for the observation of two new peaks.

One way to further confirm the rationality of the tentative explanation of the Raman spectra is based on TEM analyses, which were carried out on the as-prepared Ag_2Te sample dispersed onto a carbon-coated copper grid, after the exposure to the laser beam for 20 min during the Raman spectra measurement. As shown in Figure S1 (Supporting Information), it is very obvious that the Ag_2Te tubular nanostructures were destroyed by the laser beam, and a lot of particles appeared on the surface of Ag_2Te sample (A, B, and C). The HRTEM image (D) taken from a particle in part A of Figure S1 exposes clear lattice fringes of (1−11) the plane of the fcc silver crystal with a d spacing of 0.236 nm. The FFT pattern (inset in part D of Figure S1) can be indexed to the fcc silver crystal. X-ray EDS (F) also indicates that the particle is a silver crystal. Another HRTEM image (inset in part E of Figure S1) shows two-fringe spacing of ~0.369 nm, which may be the spacing of the (111) plane of TeO_2 (JCPDF No. 75−0882). EDS analysis (G, H) reveals that Ag_2Te on the surface of sample may be oxidized after the exposure to the laser beam for 20 min during the Raman spectra measurement.

It has been well-known that some noble metallic nanostructures can exhibit a surface-enhanced Raman scattering (SERS) phenomenon in which the scattering cross sections are dramatically enhanced for molecules adsorbed thereon.[21,22] In recent years, it was reported that even single-molecule spectroscopy is possible by SERS, suggesting that the enhancement factor can reach as much as 10^{14}−10^{15}.[23,24] The present finding indicates that such a SERS effect is achievable even via a self-generation process of nanostructures.

Studying the natural chemical character of β-Ag_2Te can help us to understand the growth mechanism of β-Ag_2Te nanotubes. The crystal structure[25] of β-Ag_2Te along the *b* and *c* axes is shown in Scheme 1. Ag(1) atoms and coordinating tellurium atoms form a sheet of tetrahedra parallel to (100), sharing four edges with other $Ag(1)Te_4$ tetrahedra. $Ag(2)Te_4$ tetrahedra are linked to two other $Ag(2)Te_4$ tetrahedra via common edges and to four $Ag(2)Te_4$ tetrahedra via common vertices in another sheet parallel to (100). The two different sheets are linked to each other via shared tetrahedron edges. The two independent silver atoms are 4-fold coordinated. Both tetrahedra are strongly distorted, although the bond distances are in the rather narrow range of 2.8415−3.034 Å. Thus, β-Ag_2Te can be seen as a layered structure. Ag(1) is in the center of the layers. The layers are parallel to (100) and are connected by Ag(2)−Te bonds. The distance between layers is about 7.5 Å [$a \sin(180 - \beta)$ Å].

(20) Kaito, C.; Nakamura, N.; Teranishi, K.; Sekimoto, S.; Shiojiri, M. *Phys. Status Solidi A* **1982**, *71*, 109.
(21) Nogueira, H. I. S.; Teixeira-Dias, J. J. C.; Trindade, T. *Encycl. Nanosci. Nanotechnol.* **2004**, *7*, 699.
(22) Kneipp, K.; Kneipp, H.; Itzkan, I.; Dasari, R. R.; Feld, M. S. *Chem. Rev.* **1999**, *99*, 2957.
(23) Kim, K.; Kim, K. L.; Lee, S. J. *Chem. Phys. Lett.* **2005**, *403*, 77.
(24) Ubbelohde, A. R. Q. *Rev. Phys.* **1957**, *11*, 246.
(25) van der Lee, A.; de Boer, J. L. *Acta Crystallogr. C* **1993**, *49*, 1444.

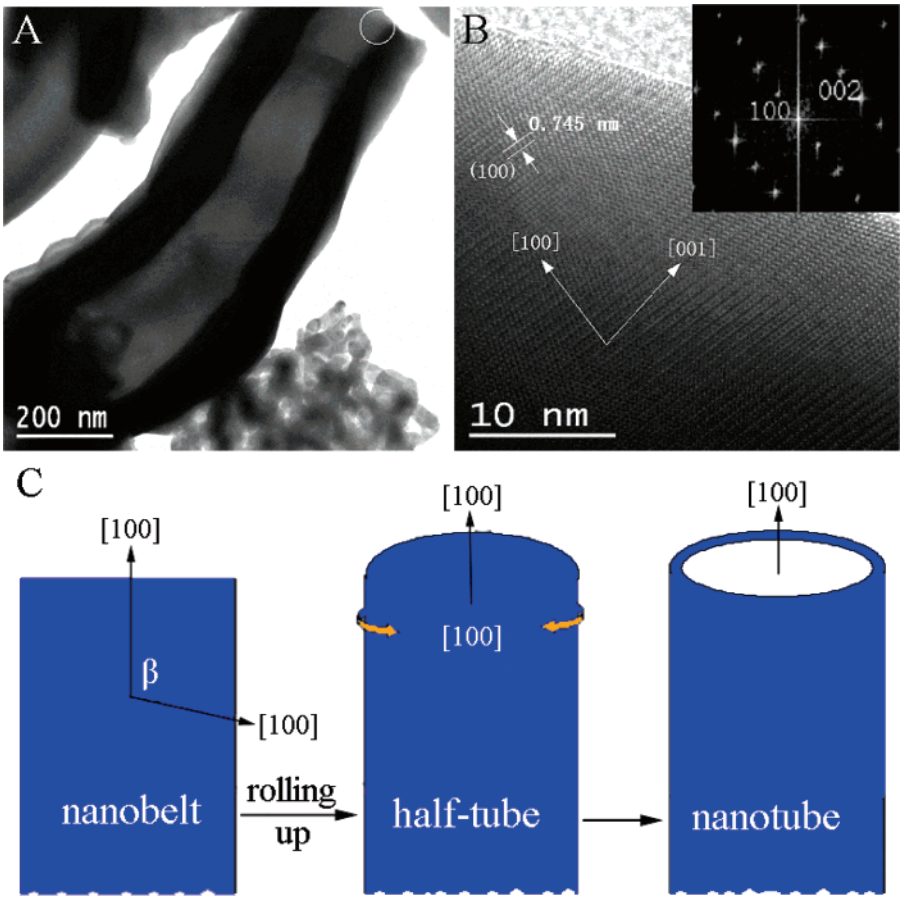

Figure 6. (A) TEM image of the individual half-tube; (B) HRTEM image and FFT pattern (inset); (C) A scheme of the formation of the Ag_2Te nanotube.

It is well-known that natural and artificial lamellar solids can be rolled up into nanotubes, under the appropriate conditions.[26−30] We believe that the rolling-up mechanism is acceptable to explain the formation of silver telluride nanotubes.

Control experiments have shown that the Ag_2Te nanobelts can change to nanotubes, under the appropriate reagent combinations and reaction conditions. The shape evolution process was followed by examining the intermediate products obtained after different reaction times. As shown in Figure S2 (Supporting Information), the products obtained after hydrothermal reactions for ∼3−4, 6−7, and more than 9 h show the morphologies of soft and curled nanobelts (A), half tubes (B), and bendy nanofibers (C), respectively. It is noted that the presence of $NH_3{\cdot}H_2O$ is necessary for the formation of Ag_2Te nanotubes. Without $NH_3{\cdot}H_2O$, only the mixture of silver and tellurium was obtained in the same reaction conditions (part D of Figure S2). The main reason may be that the ammonia acts as a transporter of the Ag^+ cations in the form of the $[Ag(NH_3)_2]^+$ cation, which is more difficult to reduce than the Ag^+ cation.

During the early stages of the hydrothermal reaction, the nanobelts formed and the existence of half-tube structures provides strong evidence for the rolling-up mechanism of the nanobelts formed. The TEM analyses on a typical half-tube further uncovered that the nanobelts curled up on the *c* axis, became half-tubes, and finally grew into nanotubes. The typical HRTEM image (part B of Figure 6) taken from an individual half-tube (indicated by the white circle in part A of Figure 6) exposes clear lattice fringes of {100} planes with a d spacing of 0.745 nm, in accordance with the distance between layers. The FFT pattern (inset in part B of Figure 6) can be indexed to the monoclinic β-Ag_2Te from the [010] zone axis and reveals that the half-tubes grow along the [001] direction of the β-Ag_2Te crystal. Thus, as shown in part C of Figure 6, we can infer that the nanotubes of as-prepared β-Ag_2Te result from the nanobelts, which appear at the early stages of the hydrothermal reaction, curl up on the *c* axis, then become half-tubes after hydrothermal reaction for ∼ 6−7 h, and finally grow into nanotubes after hydrothermal reaction for more than 9 h.

Conclusions

In summary, using the hydrothermal method, we have synthesized for the first time silver telluride nanotubes in the presence of ammonia, which is necessary for the formation of a nanotubular structure. All of these nanotubes are bendy and curled, with the diameters of 80−250 nm and more than several tens of micrometers in length. They also

(26) Schaak, R. E.; Mallouk, T. E. *Chem. Mater.* **2000**, *12*, 3427.
(27) Li, Y. D.; Li, X. L.; He, R. R.; Zhu, J.; Deng, Z. X. *J. Am. Chem. Soc.* **2002**, *124*, 1411.
(28) Chen, X.; Sun, X.; Li, Y. *Inorg. Chem.* **2002**, *41*, 4524.
(29) Xiong, Y. J.; Xie, Y.; Li, Z. Q.; Li, X. X.; Gao, S. M. *Chem.—Eur. J* **2004**, *10*, 654.
(30) Deng, H.; Wang, J. W.; Peng, Q.; Wang, X.; Li, y. d. *Chem.—Eur. J* **2005**, *11*, 6519.

show the characteristics of tubular structures with open-ended and uncovered hollow interiors. The structural phase transition of the as-prepared Ag_2Te nanotubes from the low-temperature monoclinic structure (β-Ag_2Te) to the high-temperature face-centered cubic structure (α-Ag_2Te) has been observed by DSC, TGA, and temperature-dependent XRD analysis. An interesting Raman scattering enhancement phenomenon has also been observed during the observation of Raman spectra, and a tentative explanation of this SERS phenomenon was proposed. The rolling-up mechanism of the silver telluride nanotubes is proposed to explain the tubular formation procedure based on the inherent crystal structure of low-temperature β-Ag_2Te. These anisotropic semiconductor Ag_2Te nanotubes might hold great potential applications in the engineering of nanodevices.

Acknowledgment. This work was supported by the National Science Funds for Distinguished Young Scholars of China (No. 20525310), the NSFC (No. 20463001), the Support program for 100 Young and Middle-aged Disciplinary Leaders in Guangxi Higher Education Institutions, the NSF of Guangxi Zhuang Autonomous Region (Grants 0448032 and 0640068), and the Science Foundation of Guangxi Education (Grant 200508043).

Supporting Information Available: TEM and magnified images of the as-prepared Ag_2Te sample; HRTEM images; EDS spectra showing silver, tellurium, and oxygen elements; SEM and TEM images of samples obtained by hydrothermal reaction. This material is available free of charge via the Internet at http://pubs.acs.org.

IC7006793